

# RoboTeam Twente Extended Team Description Paper for RoboCup 2024

Robin Roetenberg<sup>2,3</sup>, Mihnea Razvan Petrea<sup>1,3</sup>, Jorn de Jong<sup>1,3</sup>, Jonathan Willigers<sup>1,3</sup>, George Ayad<sup>1,3</sup>, Chris Krommendijk<sup>1,3</sup>, Bas van der Kaaden<sup>1,3</sup>, Luuk Winters<sup>1,3</sup>, Prawin Kumar Srinivasa Kumar<sup>1,3</sup>, Simone Tollardo<sup>1,3</sup>, Juan José González Torres<sup>1,3</sup>, Dario Capitani<sup>1,3</sup>, Jan Geert Kroijenga<sup>1,3</sup>, Julie Muchembled<sup>1,3</sup>, Leonie Hoekstra<sup>1,3</sup>, Csongor Buzogany<sup>1,3</sup>, Greg Ward<sup>1,3</sup>, and Moustafa Mahmoud<sup>1,3</sup>

<sup>1</sup> University of Twente (UT), Enschede, the Netherlands

<sup>2</sup> Saxion University of Applied Sciences, Enschede, the Netherlands

<sup>3</sup> RoboTeam Twente, Capitool 25 Enschede, the Netherlands

[info@roboteamtrente.nl](mailto:info@roboteamtrente.nl)

<https://roboteamtrente.nl>

**Abstract.** RoboTeam Twente has participated in the Small Size League of the RoboCup for the previous seven years. To help progress the current state of the competition the main innovations are outlined each year. This paper showcases the customized solenoids, direct drive system, the new front assembly, and the new PCBs along with the new communication system between them. Additionally, this paper will present our findings and tests related to the new flat solenoids.

**Keywords:** RoboCup · Reliability · Direct Drive · Flat Solenoids · Ball-Handling · CAN bus

## 1 Introduction

Students from the University of Twente and Saxion University of Applied Sciences make up the multidisciplinary team RoboTeam Twente. A group of students who wanted to push themselves in the robotics and artificial intelligence sectors created the team in 2016. Seven generations later, it is the responsibility of this year's team to advance the design of the preceding generations and further innovate the Small Size League (SSL) robots developed by RoboTeam Twente.

The modifications made to the hardware will be covered in this paper, starting with mechanics and finishing with electronics. An updated modular design was introduced two years ago [4], and it is expanded upon this year. A render of the robot from last year along with the render of the new robot described in this paper are shown in Figure 1 and Figure 2 respectively. The robot's specifications can be found in Table 1.

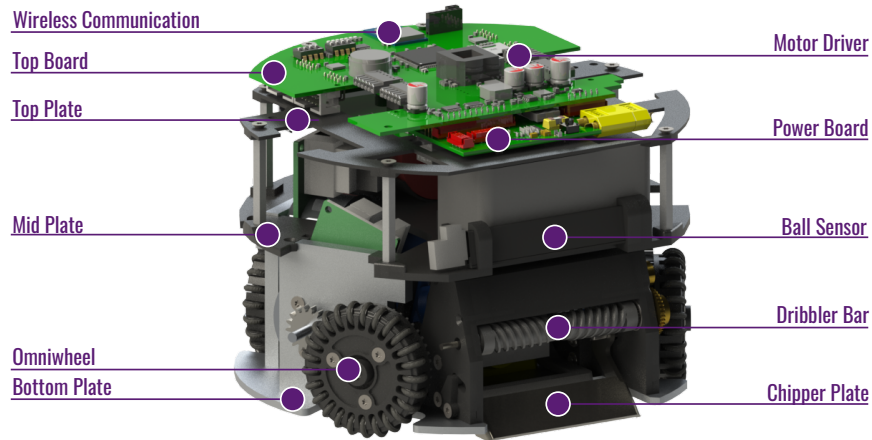


Fig. 1: Render of the 2023 version of the robot.



Fig. 2: Render of the 2024 version of the robot.

## 2 Hardware

The hardware consists of all the physical components of the robot. This is divided into mechanical and electronic parts. In recent years, RoboTeam Twente has been working on creating a more modular[4] and robust design of the hardware. This year's team will continue on that path by completely redesigning the hardware and improving the reliability of the robot. The exploded view of the new robot is shown in figure 3. For details of the new design, please take a look at our wiki.

Table 1: Robot specifications comparison

Robot Version	V2023	V2024
Dimension	$\varnothing 179 \times 149$ mm	$\varnothing 179 \times 149$ mm
Driving motor	Maxon EC-45 flat 50 Watt	ECXFL32L 48V
Dribbling motor	Maxon DCX19S EB SL 24V	Maxon DCX19S EB SL 24V
Wheel diameter	56 mm	56 mm
Wheel gear ratio	2:5	1:1
Encoder driving motors	MILE 1024 CPT	MILE 2048IMP
Dribbling bar diameter	10 mm	14 mm
Dribbling bar length	70 mm	70 mm
Encoder dribbler bar	ENX10 EASY 1024IMP	ENX10 EASY 1024IMP
Dribbler gear ratio	7:9	5:3
Microcontroller	STM32F767ZI	STM32F767ZI
Ball sensor	zForce AIR Touch	Custom Infrared sensor
Motor driver	ROHM BD63002AMUV	TI DRV8323SRTAR
Inertial Measurement Unit	Xsens MTi-3-8a7g6t	Xsens MTi-3-8a7g6t
Battery	6S1P 22.2V 150C LiPo	6S1P 22.2V 150C LiPo
Kicker-and-chipper-board Capacitor	680 $\mu$ F; Working voltage 450V	1000 $\mu$ F; Working voltage 200V
Wireless Communication	SX1280 2.4GHz	SX1280 2.4GHz

## 2.1 Mechanics

The reliability of our hardware has been a common problem over the years. This year the mechanics subteam redesigned the entire robot to improve the reliability of our Robot. This year the biggest changes are made in the transmission, kicking-chipping mechanism and ball-handling mechanism and are described below.

**Production Methods** Most of the parts are produced by one of our partners. This is all in-house designed, whereas commercially available products generally fail to meet our requirements. All of our metal parts are produced by a single partner, where the parts are made using milling, turning, drilling and laser cutting. The plunger parts are ground to lower the friction while kicking and chipping. Other parts are produced by additive manufacturing. The wheels and the front assembly are produced via SLS printing by a partner. The solenoid core and the middle and top plate are produced using an FDM printer. Furthermore, the solenoid is wounded by one of our partners.

**Direct Drive** Currently, the space at the bottom assembly is limited. This current available space is not sufficient to improve the solenoid and front assembly. A solution to create sufficient space is to use smaller motors and reduce the space needed for the powertrain assembly. A way to solve the problem of reducing the space needed for the powertrain assembly is switching to direct drive, where inspiration is gotten from TIGER's ETDP of 2020 [5].

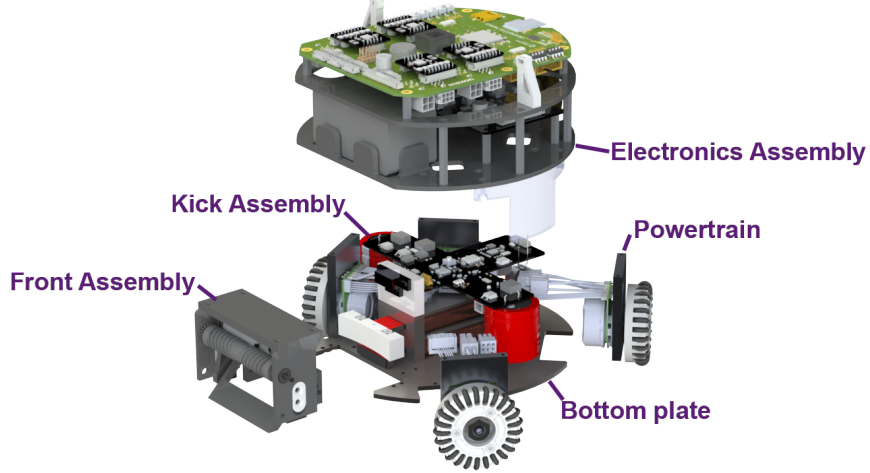


Fig. 3: Exploded view of the v2024 Robot

To switch to direct drive, a more powerful and smaller motor is needed. The more powerful motor makes the use of gears as a transmission redundant. This allows connecting the wheel directly to the motor shaft. An additional benefit of removing the gears is removing the backlash of the robot, which improves the control of the robot. A redesign of the powertrain was needed to accomplish the switch to direct drive and is shown in figure 4. The power of the motor is transferred to the wheel with the use of a form fit. A shaft connector is designed and glued using Loctite 638 to the motor shaft to create the form fit. The shaft connector is the same idea as TIGERS [5]; however, the square is bigger to provide a bigger contact area within the form fit. Furthermore, the omniwheel is redesigned, which has been used for the past seven generations. A square hole is added to the wheel main frame, see figure 4, in which the square of the shaft connector fits. Compared to the v2023 design, in which gears were used, this design will remove backlash, which will improve the control of the robot.

Due to that the motors and the powertrain assembly are smaller the wheel configuration can be changed. The configuration of the v2023 robot had an angle between the front wheels of 60 degrees and an angle of 120 degrees between the back wheels. The v2024 robot will still have an angle of 60 degrees between the front wheels; however, between the back wheels, there will be a 90-degree angle.

All of the changes result in more space at the bottom assembly. This allows for improving the solenoid and front assembly of the v2024 robot.

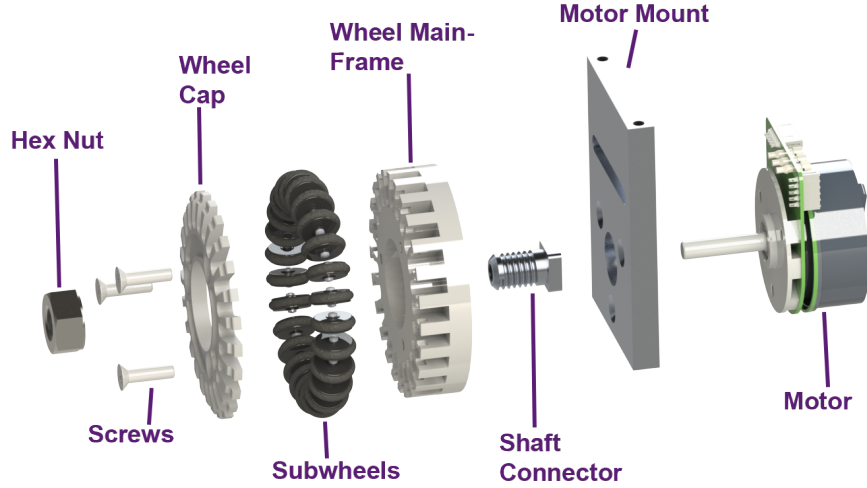


Fig. 4: The new powertrain assembly of the Robot v2024

**Solenoids** This year's mechanics team changed the round solenoids to flat solenoids. This design is inspired by TIGER's ETDP of 2020 [5]. The new solenoid will help increase the reliability of kicking and chipping the ball, where variations between different solenoids and kicker-chipper boards are observed. This is also discussed in RTT's 2023 ETDP[1]. The new design is shown in figure 5.

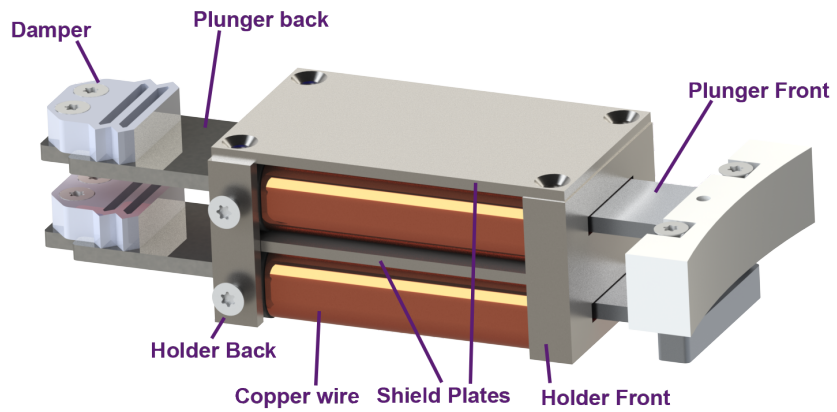


Fig. 5: New flat solenoid design

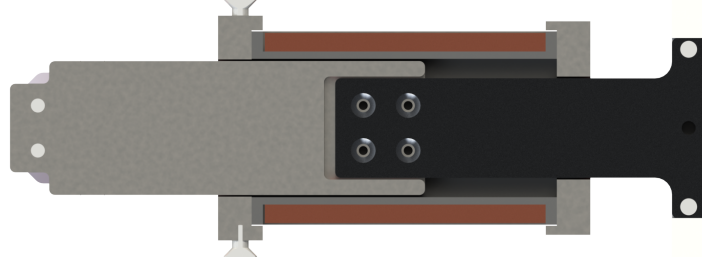


Fig. 6: Section view of the Solenoid

The design from TIGERs is adapted to our needs. The most significant change was to create a metal case around the solenoid. This is done by changing the material of the holders from aluminium to steel with a high relative permeability. Additionally, at the bottom and the top of the solenoid, a plate is added with high relative permeability. The material used is DIN 1.0503 steel, which is C45 carbon steel. This will create a sufficient metal case, which concentrates the magnetic field more towards the centre of the solenoid. Furthermore, will the new kicker-chipper experience less magnetic field compared to when using no shielding. This will help in preventing damage to the electronic boards.

In figure 7 the results of the experiment are represented. #1 represents when the solenoid has a case and the ball is placed against the solenoid, #2 represents when the solenoid has a case and the ball is placed 10 mm from the solenoid, #3 represents when the solenoid has a no case and the ball is placed against solenoid and #4 represents when the solenoid has a no case and the ball is placed 10 mm from the solenoid. Situation #2 is presented in figure 8b and #3 is presented in figure 8a. The ball speed is determined using SSL-vision, and ER-Force autoref. An average of 3 shots per scenario is taken. The test was done with 0.6 mm copper wire, which had 5 layers and a total of 342 windings.

It can be seen that placing the ball not against the plunger has the most significant increase in ball speed. Furthermore shielding the magnetic field using a case increased the ball speed compared to when no case was applied. This experiment concluded by not placing the ball directly against the plunger and applying magnetic shielding around the solenoids. The offset from the core needs more research to find the optimal setting for our new solenoid as the results do not show a clear result about the offset.

The new solenoid will make use of 0.5mm copper wire, which has 6 layers and

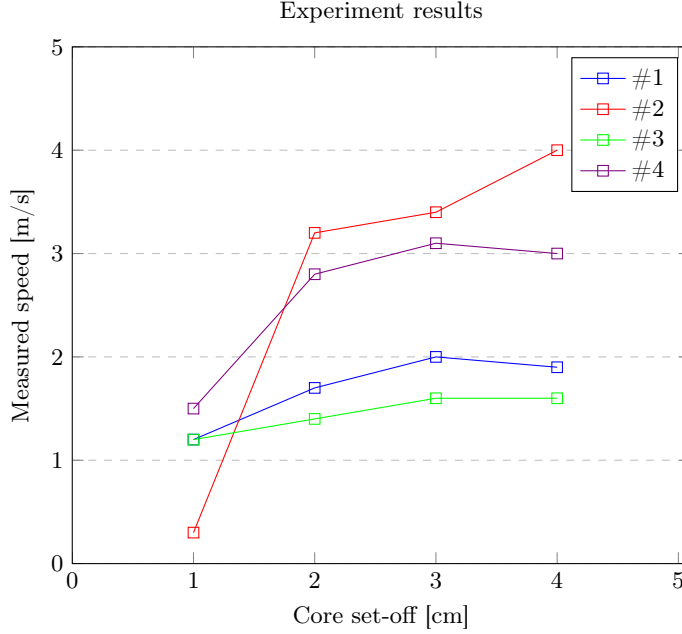


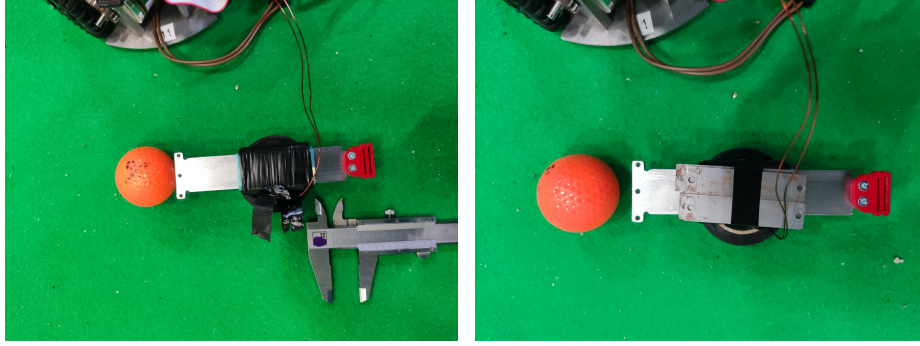
Fig. 7: Graph depicting ball speeds (of solenoid kicks) for different situations with respect to the offset of the core in cm.

a total of 546 windings. This is winded around the coil which is made from PETG. The reason for the 0.5 mm thickness is to increase the resistance of our solenoid, which makes sure the solenoid does not exceed the maximum current the kicker-chipper board can handle. A quick test concluded that similar shooting specifications were reached compared to the experiment.

**Front Assembly** Figure 9 represents the new front assembly. Inspiration for this front assembly is gotten from Tigers ETDP of 2020[5]. This front assembly will make use of a 2 Degree of Freedom (DOF) damping mechanism. This damping mechanism will make use of two flexures, which make sure the front assembly can handle the impact of an incoming ball both in vertical and horizontal directions.

The Polyurethane(PU) Rubber flexures and dribbler are moulded by custom-made ABS moulds. These moulds are vapour smoothened using acetone to ensure a smooth surface finish.

The dribbler motor is rated at 10600 rpm when no gear ratio is applied. Last year the dribbler bar could rotate at 8244 rpm, with the used gear ratio. The new robot's dribbler bar will have the ability to rotate at 17666 rpm, with a gear



(a) Solenoid without case and the ball placed against the solenoid  
 (b) Solenoid with case and the ball placed 10mm in front of the solenoid

Fig. 8: Two experimental setups for the solenoid test

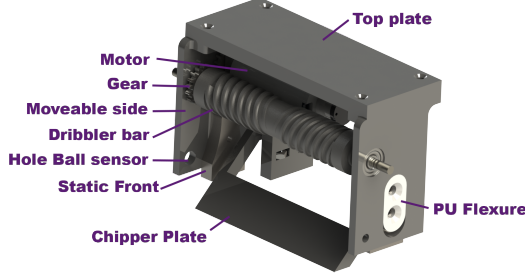


Fig. 9: The new Front Assembly

ratio of 5:3. During a simple test, where the gears of the old robot were swapped places, it was concluded that increasing our dribbling speed instead of lowering helped in receiving the ball and moving the ball towards the centre.

As the rule states the ball coverage should be at a maximum of 20%. The new front assembly is designed to have a maximum ball coverage of 19%.

$$A\% \pi R^2 = R^2 \arccos\left(1 - \frac{h}{R}\right) - (R - h) * \sqrt{(R^2 - (R - h)^2)} \quad (1)$$

Equation 1 is solved using the symbolic solver of MATLAB. Representation of the symbols of equation 1 are given in figure 10. This concluded the height should be at 43.625 mm, which is calculated using Pythagoras.

Our last ETDP [1] stated the chipper bar is used to add a third point of contact. This was inspired by the ETDP of Zjunlict [3], which improves ball-handling skills compared to a two-point contact model. After the RoboCup, it was con-

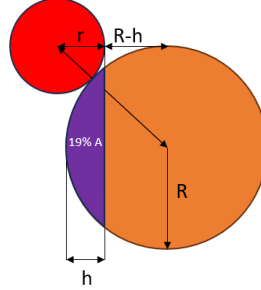


Fig. 10: Sketch for determination of the height of the dribbler

cluded the implementation was not successful. The chipper bar prevented the ball from contacting the dribbler bar, where the ball-handling skills were decreased. This year more research has been put into reading the ETDP of Zjunlct [3], looking at the model v2020 of TIGERS[5] and the ETDP of RoboCIn[6]. The new chipper bar focuses on enabling the dribbler bar to still touch the ball.

**General Changes** To fit the new electronics boards on the bottom assembly, the middle and top plates are adjusted. Mainly the screw holes are relocated to place the electronic PCBs and holes are created to guide the wires of all the boards and motors. Also, a cover is added to shield the capacitors to increase the safety of handling the robot by preventing the capacitors from being easily touched. All the details of our changes, such as technical drawings, will be made available at our wiki before the 2024 RoboCup.

## 2.2 Electronics

This year a complete redesign of the system is being undertaken. Current hardware has issues regarding reliability. This causes unwanted delays in design progression as time is spent making repairs. This process takes longer than necessary due to a lack of debugging functionality. This is something that we aim to improve upon in our new designs. Finally, we encountered a design bottleneck regarding hardware upgrades. This year we decided to create hardware that can be upgraded at a later stage. This could be in the form of additional hardware or a redesign of any current hardware. Regardless of the desired change, this can be done without having to completely redesign the entire system. Some finished (and already partially working) designs are included to give the reader a visualisation of how we implement our improvements and to show case the design standards we have put in place in the new hardware.

**New motor driver connectors** The motor driver connector will be replaced by two, two-row connectors; the motor driver connector sockets are now placed

on the face of the motherboard as opposed to the sides. This way, the motor driver will be fully supported. The connectors also have a larger number of pins making the connection between the head and socket much stronger. This drastically lowers the possibility of them coming loose due to vibrations.

The cables required for the motor driver will now be connected to the top board rather than the motor driver itself. This acts to reduce the potential force acting on the motor driver board. The movement of the motor driver relative to the top board is now almost completely restricted. Additional screws could also be used in future to restrict this movement completely. All in all, the new design improvements have led to a much more secure connection between the motor driver and the top board. A concept render is shown in figure 11.



Fig. 11: A rendered model displaying the new motor driver connectors.

**Isolated Board design** All boards have been redesigned with their own MCU. Each board can then communicate via a CAN 2.2 bus with the motherboard. The boards can now operate in isolation, thus, the system is now truly modular. This in turn improves reliability as malfunctions are contained in isolated areas and cannot damage more sensitive or more important parts of the system (the IMU for example). Debugging functionalities can now be used to detect from which sub-systems and errors occurred making maintenance all the more straightforward. An additional benefit is the freedom of redesigning each board independently as now no parts of the system are dependent on another sub-system.

**Boundary Scanning (JTAG)** The issue of soldering mistakes is something addressed in the redesign. JTAG (Joint Test Acces Group) allows for boundary scanning. This is a process that uses features already present in most chips (in the case of the hardware all MCUs have JTAG capabilities) to send and receive test signals along all traces to determine continuity. A software interface then allows for easy identification of any present soldering mistakes.[8]

The addition of JTAG also yields another improvement: namely a better programmer connection. Currently, a custom connector allowing for programming and serial readout is used. This has been replaced by the standard JTAG connection which has the same functionality (and extra) as before. This has the

advantage of improving hardware usability and aesthetics (these are important admittedly).

**Debugging** Now the importance of debugging should be clear - debugging functionality on the current hardware is scarce. It is also of little help when trying to diagnose precise hardware malfunctions. For these reasons, additional debugging functionality has been included.

An OLED display has been implemented atop the motherboard; the OLED screen displays a menu that allows for debugging of hardware. The user interface for this is a combination of buttons and dip switches. The menu allows for precise detection and testing of hardware components without the necessity of a computer and time to prepare diagnostic programs. The menu can also display diagnostic information (ID, battery level, role etc.), allow for control parameter changes, display software debugging variables and more. It allows for much more extensive debugging functionalities to be available on the Robots themselves.

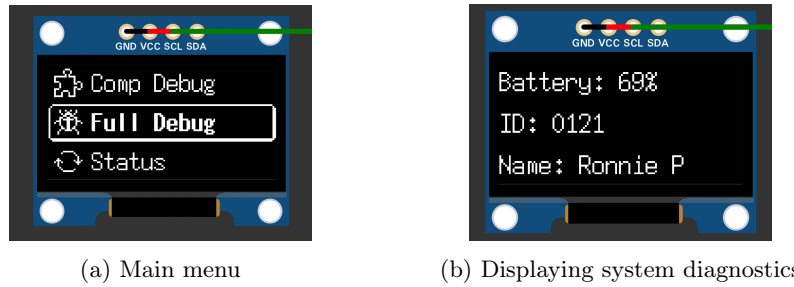


Fig. 12: Simulated rendition of the OLED display menu concept.

Additional test points have also been placed on the PCBs. These are placed at the areas following a likely malfunctioning area. This is commonly at IC outputs or high voltage/current handling components. This allows for a quick diagnosis with a multi-meter to test basic functionality.

**Shared Bus** To fix the upgradability problem, it was decided to connect all the boards using the CAN bus. Not only does this allow for upgradability, the modular system design 2.2 is also realised in this fashion. CAN (Controller Area Network) is a serial, slave-less communication protocol. It has the benefit of being resistant to noise and interference; it uses a differential signal pair cancelling out common-mode signals along the wires. This is crucial as noisy signals can lead to system malfunctions; the Robot will not perform optimally in this case (actuation signals could be corrupted by noise and, therefore, not have their intended effect for example). Each board can now send and receive information via their MCU. A priority system can be implemented to determine which signals are communicated first to avoid collisions.[2]

Each board now can work in isolation, making control over the Robot's components more direct and local. This should improve the response time of our Robot as we remove any delays introduced by parasitic effects (due to signals having to travel larger than necessary distances). The shared bus only uses two pins for communication so the connector has been designed to include a power trace. This will directly supply the CAN transceiver chip, keeping the system compact and robust (a CAN connection does need an extra 5v supply from the board it is placed on). Upgradability is now possible; new boards require only a CAN connector (and relevant traces to its MCU) to be integrated with the system.

The new motherboard has six available CAN ports as shown in figure 13. An adapter board with extra CAN ports could be implemented if this proves too few.

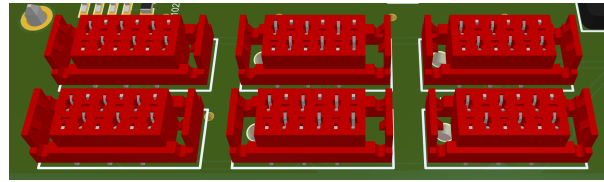
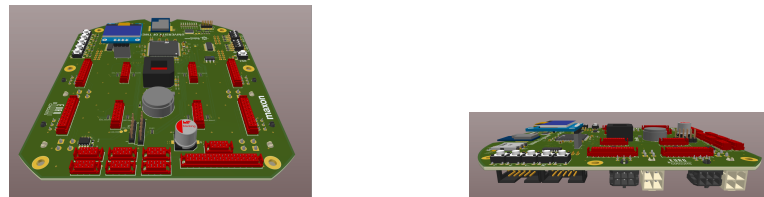


Fig. 13: A rendered 3D model of the new CAN ports atop the motherboard.

**New Mother Board** This is the central module of the system. The main processor, wireless communication and IMU are all located here. The motherboard collects all data from the system sensors and relays this to the controlling algorithm via the wireless communication module. Any received instructions are also actuated via the motherboard. There are many differences between the old and new renditions. Figure 14 depicts a 3D model of the new motherboard from different perspectives. A top-level diagram of the motherboard showing its subsystems and their interconnections is given in figure 15.



(a) Top side

(b) Side view displaying connector ports.

Fig. 14: The rendered 3D model of the new Mother Board design.

One evident change is the board shape. The curvature and dimensions are similar to the previous edition as the Robot's dimensions have not been altered. The cut-outs present in the old design have been filled; the new motor drivers have been mounted to the motherboard's surface to improve connection security. Noticeable also, is the cut-out beneath the antennae of the wireless chip. This allows the antenna to radiate in a full (as opposed to half) plane space as there is no (potential) termination of the electric field due to the PCB being directly below it. This is of course non-ideal as unobstructed emission is desired for better transmission efficiency.[7]

The addition of an OLED display allows for onboard diagnostics. This acts to improve debuggability; it also has the benefit of making this process simpler - there is a visualisation of diagnostics making it now possible for other sub-teams to test hardware (the old probe and schematic method is redundant). Additional buttons have been added to give control over the menu shown on the OLED display. To further our testing capabilities, a JTAG connection interface has been added. This allows for the discussed boundary scanning methods to be applied; it is also the interface with which the MCU logic can be programmed. Now, this is present on all boards presented in this section. As such, other board sections will only mention this briefly.

Extra connectors for the CAN and I2C buses are also available. This allows for extra peripheral devices to be added at will. The CAN connectors are used to interconnect all PCBs in the system via the CAN bus to the central MCU. This is what makes upgradability and true modularity possible. The I2C pins were previously used for a UART interface for serial feedback from the MCU. These have been repurposed to allow for connection with other peripheral devices: a speaker for example. Furthermore, the Motor driver connection was changed from the side to a top mount configuration - connection to the motor itself was added to the underside of the motherboard as opposed to the motor driver itself.

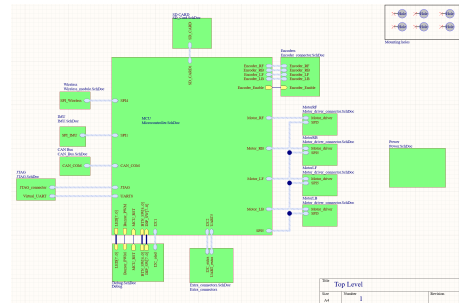


Fig. 15: A top-level diagram showing the subsystems of the motherboard and how they interconnect.

**New Power Board** The power board acts as the power distribution centre. Connection of the supply battery to the system takes place here. Extensive changes have been made to the old revision of the power board. In figure 16 a 3D model of the new power board is shown. The top-level diagram of the power board's sub-systems and their interconnections is displayed in 17.

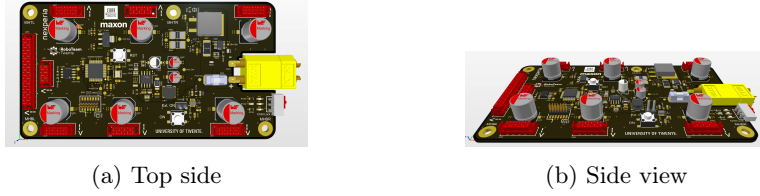


Fig. 16: The rendered 3D model of the new Power Board design.

The power board is populated with many more components than the previous edition. An MCU present on the board allows for the mentioned isolated board design concept to be realised. Control and processing of the onboard ICs and sensors is managed by this MCU. This in turn communicates with the central MCU via the CAN bus 2.2 to send or receive instructions or diagnostic information. Thus, the modular design of the system is actualised using this design method.

The board itself has another functionality: protection of the board from supply fluctuations. Therefore, chips (a hot swap converter) are put in place to protect against over-current and reverse polarity. This chip is now directly connected to the powerboard's MCU ensuring that any potential supply malfunctions will have effects isolated only to the power distribution part of the system.

The additional power connectors are to allow for the connection of new hardware; this matches the number of CAN connectors. A separate motherboard power connection is also present. To remove components from the motherboard and improve system modularity the Buck converter is now placed on the power board. The voltage it converts (24V–5V) is required on the motherboard (the motherboard, in turn, distributes this 5V to other boards via the CAN connection) and is more logically placed on the power board. The buck converter is also subject to regular malfunction so is better placed on a different board to isolate the issue to a smaller, more easily replaceable (the motherboard contains a larger number of and more expensive components) part of the system.

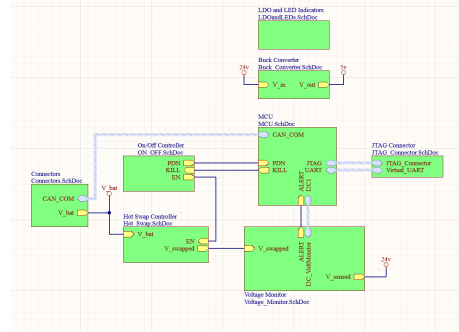


Fig. 17: A top-level diagram showing the subsystems of the power board and how they interconnect.

## References

1. Andringa, J., Bink, T., Bojkow, B., Bojorge-Alvarez, J., Born, H.V.D., Doornkamp, C., Ganzeboom, E., Javed, U., Meulenkamp, T., Steerneman, E.: Roboteam twente extended team description paper for robocup 2023, <https://roboteamtwente.nl>
2. Circuits, A.A.: Introduction to CAN. <https://www.allaboutcircuits.com/technical-articles/introduction-to-can-controller-area-network/> (2019)
3. Huang, Z., Chen, L., Li, J., Wang, Y., Chen, Z., Wen, L., Gu, J., Hu, P., Xiong, R.: Zjunlct extended team description paper for robocup 2019 (2019). <https://doi.org/10.48550/ARXIV.1905.09157>, <https://arxiv.org/abs/1905.09157>
4. Monat, C., Dankers, E., Skurule, K., Steenmeijer, L., Sijtsma, S., Diamantopoulos, S., Aggarwal, R., Smit, T., van Harten, A.: Roboteam twente extended team description paper for robocup 2022 (2022), [https://ssl.robocup.org/wp-content/uploads/2022/04/2022\\_ETDP\\_RoboTeam-Twente.pdf](https://ssl.robocup.org/wp-content/uploads/2022/04/2022_ETDP_RoboTeam-Twente.pdf)
5. Ryll, A., Jut, S.: Extended team description for robocup 2020 (2020), <https://tigers-mannheim.de>
6. Silva, C., Alves, C., Silva, E., Martins, F., Cavalcanti, L., Maciel, L., Vinícius, M., Monteiro, J.G., Moura, P., Cruz, J.V., Santana, P.H., Sousa, R., Rodrigues, R., Fernandes, R., Morais, R., Araújo, V., Silva, W., Barros, E.: Robôcin extended team description paper for robocup 2022, <https://robocin.com.br/>
7. Solutions, C.P.: Antenna Design Principles for PCB Designers. <https://resourcespcb.cadence.com/blog/antenna-design-principles-for-pcb-designers> (2021)
8. Technologies, J.: Boundary Scanning. <https://www.jtag.com/boundary-scan/> (1993)